Theoretical Studies of the Kinetics of Planar–Tetrahedral Equilibration in Nickel(II) Complexes. 1. Reaction Coordinates and Potential Energy Surfaces

Lawrence L. Lohr, Jr.

Contribution from the Department of Chemistry, The University of Michigan, Ann Arbor, Michigan 48109. *Received May 23, 1977*

Abstract: A series of theoretical studies of the kinetics of the equilibration of planar spin-singlet and tetrahedral spin-triplet complexes of Ni(II) is begun by the introduction of global bending coordinates for four-coordinate species. Potential energy surfaces for singlet and triplet levels are calculated both with and without spin-orbit coupling as a function of these coordinates using a crystal-field model. The results are discussed in terms of their relevance to surface "hopping", which is treated in detail in the second article of the series.

I. Introduction

It is now well established that several important classes of metal coordination complexes are characterized by stereochemically nonrigid molecular structures. The best known systems of this type are certain four-coordinate complexes with one or two bidentate ligands and certain six-coordinate complexes with one, two, or three bidentate ligands. Unidentate ligands complete the coordination spheres as required by the coordination numbers. Evidence for the ligand site interchanges characteristic of nonrigidity has largely come from dynamic nuclear magnetic resonance spectroscopy (DNMR), a technique which has proven to be invaluable in this area. The use of this method has been described in a series of excellent review articles on the stereochemistry of nonrigid complexes. These include the reviews by Holm and O'Connor,[1] Holm and Hawkins,[2] Pignolet and LaMar,[3] Pignolet,[4] and Holm.[5]

In one of the most recent of these reviews, Holm[5] defines a stereochemically nonrigid complex "as one which manifests exchange line-broadening or achieves the fast exchange limit within the temperature interval of ca. −100 to 200 °C usually accessible in NMR measurements of adequately soluble and thermally unstable compounds." He further labels these as "fast" to emphasize their intramolecular lability which under ordinary conditions prevents separation of isomers. Thus their rearrangement kinetics are determined from rates of interconversion at equilibrium. By contrast stereochemically rigid or "slow" complexes are those which have not shown DNMR behavior in the accessible temperature interval, so that their rearrangement kinetics are obtained by the more conventional methods which monitor rates of approach to equilibrium.

An important class of stereochemically nonrigid complexes are the four-coordinated complexes of Ni(II) formed from either two bidentate ligands or from one bidentate ligand and two unidentate ligands. It has been well known for some time that many of these complexes are characterized by a thermal equilibrium between a "planar" spin-singlet species and a "tetrahedral" spin-triplet species,

$$\text{planar } (S = 0) \rightleftharpoons \text{tetrahedral } (S = 1) \qquad (1)$$

with the equilibrium constant for eq 1 being of the order of unity at room temperature. We follow the established custom of using the term "tetrahedral" to refer to the twisted equilibrium geometry of the paramagnetic species, even though the actual molecular symmetry can be no higher than D_{2d} for the twisted structure of bisbidentate complexes with symmetric ligands. Bisbidentate complexes showing this behavior include those with anionic ligands derived from aminotroponeimines, salicylaldimines, and β-keto amines. While the electronic absorption spectrum of a solution containing such a complex is the superposition of absorption spectra of the singlet and triplet species, with relative intensities varying with temperature in accord with a Boltzmann distribution, the ^{1}H NMR spectrum is typically a dynamically averaged spectrum combining that due to singlet and triplet species, with the position of the signals varying with temperature in accord with a Boltzmann distribution. Thus the lifetime τ of a given spin state has usually been estimated as being within the bounds $\tau \geq 10^{-13}$ s and $\tau \leq 10^{-4}$–10^{-6} s.

A number of complexes of Ni(II) with phosphine ligands have been studied by NMR,[6-11] and one of these, Ni(dpp)Cl_2, has also been studied by a photochemical perturbation experiment.[12] Solutions of the complex were irradiated with a Q-switched neodymium laser at either 1060 nm or 530 nm, with the absorbance monitored in the range 375–530 nm. Initial rapid changes in absorbance were followed by the slower reestablishment of thermal equilibrium between planar and tetrahedral species. Rate constants obtained for reaction 1 are $k_f = 4.5 \times 10^5$ s^{-1} and $k_r = 6 \times 10^5$ s^{-1}, which are in the range of those estimated from NMR data for the Ni(dpp)X_2 complexes. The relationship between decay time constants appropriate to a chemical relaxation experiment, such as that described above, and spin-state lifetimes is described in the following article.[13] It should also be noted that early estimations of thermodynamic parameters for eq 1 from NMR data did not take into account the orbital degeneracy that nearly obtains for the lowest spin-triplets of Ni(II) in a distorted tetrahedral field. This degeneracy was considered by McGarvey[14] in his theoretical treatment of contact and dipolar shifts.

It is at first glance surprising that the rate of the interconversion 1 is so rapid, since it involves not only a change in spin-state but also a significant change in geometry. Holm has recently stated[5] that "the origin of the extremely low barrier for the planar-tetrahedral interconversion of Ni(II) complexes is not understood nor is the mechanism of this interconversion known". He presented arguments in support of a non-bond-rupture pathway involving a diagonal twist, which also serves as a racemization pathway between Δ and Λ forms of "tetrahedral" Ni(L-L′)$_2$ complexes with asymmetric bidentate ligands L-L′. In a simple application of Woodward-Hoffmann[15] arguments, Eaton[16] suggested that the process was fast simply because it was "orbitally allowed." In a more rigorous analysis, Whitesides constructed[17] qualitative state correlation

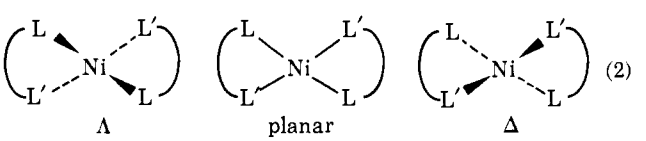

(2)

0002-7863/78/1500-1093$01.00/0

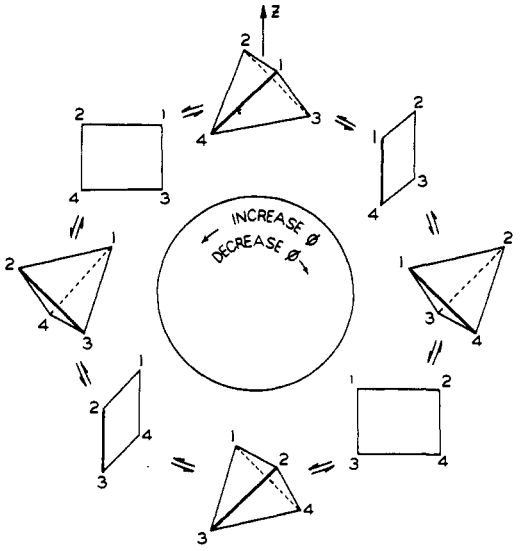

Figure 1. Molecular structures for ML_4 generated by variation of the polar angle θ at a fixed value of $\Phi = \pi/4$. See Table I.

Table I. Ligand Coordinates for D_2 Symmetry of ML_4 Complexes

Ligand	R	θ	Φ
1	R	θ	Φ
2	R	θ	$\Phi + \pi$
3	R	$\pi - \theta$	$-\Phi$
4	R	$\pi - \theta$	$-(\Phi + \pi)$

diagrams and showed that the process is not thermally allowed in that the ground state of the planar complex does not correlate with the ground state of the tetrahedral complex. The question of the nature of the interconversion process was then left open.

It is the purpose of this and the following article[13] to examine theoretically the nature of the interconversion process (eq 1). The emphasis is on the construction of a theoretical framework within which to visualize the process and to formulate questions as to the factors influencing the interconversion rates. We provisionally assume that the interconversion proceeds by a "curve hopping" process without the breaking of bonds, and then explore the implications of such an assumption to see if it is compatible with the observations. Thus we assume the process to be associated with deformation paths such as the twisting motion shown in eq 2. The theoretical approach outlined in this series of articles should be applicable as well to other spin equilibration reactions, such as that between singlet and quintet states of six-coordinate Fe(II).[18]

II. Reaction Coordinates

The Born-Oppenheimer approximation[19] divides the description of a chemical process into two stages: a consideration of the total electronic energy as a function of geometry, leading to a potential energy surface for each electronic state, and a consideration of the motion of the nuclei, with the electrons following, on a given surface or possibly from one surface to another. In order to describe the planar-tetrahedral interconversion in as broad a perspective as possible, we consider a four-coordinate complex ML_4 with unspecified unidentate ligands. The relevant vibrational modes are the degenerate e bending modes of a T_d structure (3a) or the out-of-plane b_{1u} bending mode and the inplane b_{1g} bending mode of a D_{4h} structure (3b). The "plus" and "minus" signs in (3) denote displacements up and down, respectively. The components of

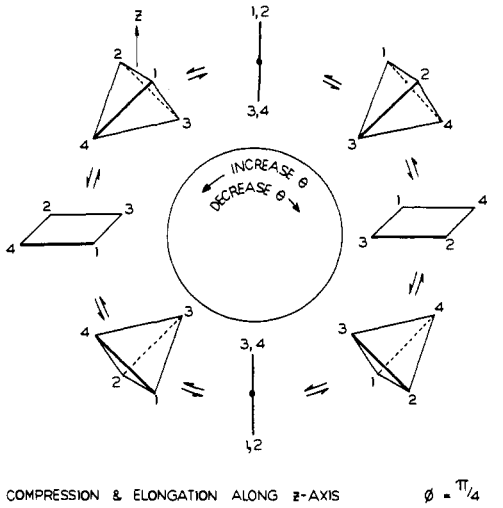

Figure 2. Molecular structures for ML_4 generated by variation of the twist angle Φ at a fixed value of $\theta = \theta_0 = \cos^{-1}(3^{-1/2})$. See Table I.

the e bending mode labeled $3z^2 - r^2$ and $x^2 - y^2$ are sometimes designated as S_{2a} and S_{2b}, respectively. The labeling of the D_{4h} modes is that appropriate for ligands lying *between* the x and y Cartesian axes rather than *on* these axes.

(3a)

(3b)

Table I gives the spherical polar coordinates of the four ligands in terms of a bond length R and the angles θ and Φ. Figure 1 displays the compression and elongation along the z axis of the complex implied by variation of θ at a fixed value of $\Phi = \pi/4$, while Figure 2 displays the twist about the z axis implied by a variation of Φ at a fixed value of $\theta = \theta_0 = \cos^{-1}(3^{-1/2})$, which is one-half of the tetrahedral angle. Since we are considering R to be constant, it is very useful to visualize the various structural transformations of an MX_4 complex as the motion of a point on the surface of a sphere. For arbitrary θ and Φ the molecular symmetry is D_2, but we note the occurrence of the following special symmetries:

$$\begin{aligned}
&\theta = 0 \text{ or } \pi,\ \Phi \text{ undefined:} && D_{\infty h} \\
&\theta = \pi/4 \text{ or } 3\pi/4: && D_{4h} \text{ for } \Phi = 0, \pi/2, \pi, \text{ or } 3\pi/2 \\
& && D_{2d} \text{ for } \Phi = \pi/4, 3\pi/4, 5\pi/4, \text{ or } 7\pi/4 \\
&\theta = \theta_0 \text{ or } \pi - \theta_0: && D_{2h} \text{ for } \Phi = 0, \pi/2, \pi, \text{ or } 3\pi/2 \\
& && T_d \text{ for } \Phi = \pi/4, 3\pi/4, 5\pi/4, \text{ or } 7\pi/4 \\
&\theta = \pi/2: && D_{\infty h} \text{ for } \Phi = 0, \pi/2, \pi, \text{ or } 3\pi/2 \\
& && D_{4h} \text{ for } \Phi = \pi/4, 3\pi/4, 5\pi/4, \text{ or } 7\pi/4
\end{aligned} \qquad (4)$$

Thus there are in this configuration space 6 $D_{\infty h}$ structures at the vertices of an octahedron, 8 T_d structures at the vertices of a cube, and 12 D_{4h} structures at the vertices of a cube-octahedron. Figure 3 displays a view looking down the z axis of the upper hemisphere of this configuration space. The $D_{\infty h}$ structures correspond to the linear triatomic molecules formed by the coalescing of ligand pairs to form single ligands. The molecular potential energy, of course, goes to infinity at these points. The six structures arise from the three ways of coales-

cing ligands, namely, (1,2) and (3,4), (1,3) and (2,4), and (1,4) and (2,3), combined with two orientations of each. That is, the $D_{\infty h}$ structures on the $\pm x$ axis have the same ligands coalesced, but differ by a rigid body rotation of π. The eight T_d structures arise from four orientations for each of the two "isomers" possible with numbered ligands. Specifically the "cube" of T_d structures consists of a "tetrahedron" of four orientations of one isomer and a complementary "tetrahedron" of four orientations of the other isomer. Finally the cube-octahedron of 12 D_{4h} structures involves three isomers, namely, with trans ligands (1,2) and (3,4), (1,3) and (3,4), and (1,4) and (2,3); it is constructed from "squares" of four orientations of a given isomer, with one isomer in each of the planes $x = 0$, $y = 0$, and $z = 0$. Each T_d structure has three D_{4h} "nearest neighbors", while each D_{4h} structure has two T_d "nearest neighbors"; the number of T_d and D_{4h} structures is inversely proportional to their symmetry numbers of 12 and 8, respectively. Structural interconversions will take place along or close to circular arcs lying in (110) planes, thus avoiding the $D_{\infty h}$ structures on (100) axes.

We note the parallelism between the present problem and the XeF_6 pseudorotational problem which we earlier investigated[20] in detail using a crystal-field model. As pointed out by Bartell and Gavin,[21] the instability of octahedral XeF_6 is largely along the t_{1u} bending coordinates. Choosing these in a spherical polar coordinate representation, and considering a constant radial displacement from O_h symmetry, the pseudorotational motion may be described as a motion of a mass point on the surface of a sphere. There are 6 C_{4v} structures along (100) axes, analogous to the 6 $D_{\infty h}$ structures for ML_4, 12 C_{2v} structures along (110) axes analogous to the 12 D_{2h} structures for ML_4, and 8 C_{3v} structures along (111) axes analogous to the 8 T_d structures for ML_4.

The appearance in the configuration space of Figure 3 of differently oriented but otherwise identical structures reflects the well-known coupling in molecules between internal rotation and overall rotation. This coupling has been extensively discussed for ethane and related molecules.[22] It should also be noted that a detailed description of the relevant internal motions in a complex of the $M(L\text{-}L)X_2$ type requires *two* polar angles and one twist angle, thus defining a three-dimensional configuration space. However, for our present purposes we shall consider only the two-dimensional space described above. We note that the simple twisting motion of a bisbidentate complex with a bite angle of 2θ corresponds to circular motion in Φ as in Figure 2, but with the appropriate θ value. Bidentate ligands essentially preclude planar-tetrahedral interconversion through θ motion as in Figure 1. Thus the process 1 for $Ni(L\text{-}L)_2$ and $Ni(L\text{-}L)X_2$ complexes will be formulated in terms of hindered internal rotation through Φ, with curve hopping from spin-singlet potential energy curves to spin-triplet potential energy curves.

III. Potential Energy Surfaces

We now consider the "global" potential energy as a function of θ and Φ for both spin singlets and triplets. Two approaches are used: first, the choice of a convenient analytic form for the potential, with parameters related to experimental data; and second, the calculation of potential energy surfaces by an extended crystal-field method including a multiplet structure calculation.

The empirical approach is similar to that recently employed by Pitzer and Bernstein,[23] who constructed a surface for XeF_6 using infrared, electron diffraction, and molecular beam deflection data. A comparison of calculated and observed third-law entropies served as a check on the results. However, we do not have as much data at our disposal, and, in addition, we have the problem of constructing several intersecting surfaces. For the ML_4 complex of D_2 minimal symmetry we note that the potential energy in the θ and Φ coordinates of section II must have O_h symmetry. A form which has extrema for the 12 D_{4h} structures occurring along (110)-type axes is

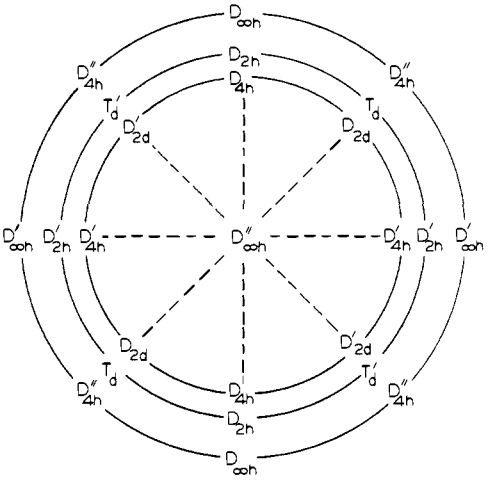

Figure 3. View looking down the z axis of the upper hemisphere of the configuration space define by θ and Φ in Table I. The molecular symmetry is D_2 in general, with special symmetries denoted by the appropriate symbols. The outer rim corresponds to the equatorial plane defined by $\theta = \pi/2$.

$$V(\theta, \Phi) = A\{Y_{6,0}(\theta, \Phi) - (7/2)^{1/2}[Y_{6,4}(\theta, \Phi) + Y_{6,-4}(\theta, \Phi)]\} \quad (5)$$

where the $Y_{L,M}(\theta, \Phi)$ are the standard spherical harmonics and A is a constant. This is a familiar form in the cubic crystal-field splitting of the energy levels of rare-earth ions, and has values [in units of $(13/\pi)^{1/2}A$] of $\frac{1}{2}$ along a (100) axis, $-\frac{13}{16}$ along a (110) axis, and $\frac{8}{9}$ along a (111) axis. If we assume such a surface with $A > 0$ for a spin-singlet, and another such surface with a trace added and with $A < 0$ for a spin-triplet, we can fit A and the trace to an adiabatic energy difference and an activation energy (taken as the energy of intersection of the surfaces). We describe a simplified calculation of this style in the following article.[13]

As an introduction to our crystal-field calculations, we list in Table II certain symmetry correlations for ML_4 complexes of d^8 ions with unidentate ligands. These correlations, as well as those in Tables III and IV described below, are obtained by adaptation of tables given by Wilson, Decius, and Cross[24] and by Herzberg.[25] Listed are only those levels both with and without spin-orbit coupling, which arise from the lowest spin-singlet, $^1A_{1g}$, in D_{4h} symmetry, and the lowest spin-triplet, $^3T_1$, in T_d symmetry. We note under B-2 of Table II that spin-orbit coupling in complexes of D_2 symmetry produced by rotation through Φ mixes the spin-singlet with the $J = 0$ level of $^3T_1$ and both low-symmetry components of the tetrahedral E component of the $J = 2$ level of $^3T_1$. However there is no mixing of the spin-singlet with the $J = 1$ levels or the T_2 components of the $J = 2$ levels. Examination of the symmetries of *all* of the 45 states arising from d^2 or d^8 configurations shows that the irreducible representations with spin-orbit coupling in D_2 symmetry are

$$\Gamma(D_2) = 15A + 10B_1 + 10B_2 + 10B_3 \quad (6)$$

The same D_2 symmetry obtains for the idealized bisbidentate complex, the symmetry correlations for which are given in Table III. Correlations for complexes with one bidentate and two unidentate ligands, $M(L\text{-}L)X_2$, are given in Table IV, in which we note that with the spin-orbit coupling in the C_2 symmetry appropriated to a twisted complex, one component

Table II. Symmetry Correlations for ML_4 Complexes of d^8 Ions with Unidentate Ligands

T_d	$D_{2d}(z)$	$D_{4h}(z)$
A. No Spin-Orbit Coupling		
1. Bending Mode E(θ) of T_d or B_{1u} of $D_{4h}(z)$		
$^3T_1$	$^3A_2 + {}^3E$	$^3A_{2g} + {}^3E_g$
$^1A_1$	$^1A_1$	$^1A_{1g}$
2. Bending Mode E(ϵ) of T_d		
T_d	D_2	D_{2h}
$^3T_1$	$^3B_1 + {}^3B_2 + {}^3B_3$	$^3B_{1g} + {}^3B_{2g} + {}^3B_{3g}$
$^1A_1$	^1A	^1A_g
3. Bending Mode B_{1g} of $D_{4h}(y)$		
$D_{2d}(z)$	D_2	$D_{4h}(y)$
$^3A_2 + {}^3E$	$^3B_1 + {}^3B_2 + {}^3B_3$	$^3A_{2g} + {}^3E_g$
$^1A_1$	^1A	$^1A_{1g}$

		T_d	$D_{2d}(z)$	$D_{4h}(z)$
B. With Spin-Orbit Coupling				
1. Bending Mode E(θ) of T_d or B_{1u} of $D_{4h}(z)$				
$^3T_1$	($J = 2$)	T_2	$B_2 + E$	$B_{2g} + E_g$
		E	$A_1 + B_1$	$A_{1g} + B_{1g}$
	($J = 1$)	T_1	$A_2 + E$	$A_{2g} + E_g$
	($J = 0$)	A_1	A_1	A_{1g}
$^1A_1$		A_1	A_1	A_{1g}

		T_d	D_2	D_{2h}
2. Bending Mode E(ϵ) of T_d				
$^3T_1$	($J = 2$)	T_2	$B_1 + B_2 + B_3$	$B_{1g} + B_{2g} + B_{3g}$
		E	2A	$2A_g$
	($J = 1$)	T_1	$B_1 + B_2 + B_3$	$B_{1g} + B_{2g} + B_{3g}$
	($J = 0$)	A_1	A	A_g
$^1A_1$		A_1	A	A_g

of each T_1 or T_2 level has the same symmetry as the totally symmetric spin singlet, so that the 45 levels yield

$$\Gamma(C_2) = 25A + 20B \tag{7}$$

With no molecular symmetry at all, as actually obtains in some of the complexes, all 45 states are mixed together. However, for illustrative purposes we shall confine ourselves to the idealized D_2 symmetry of section II. Even so there are not just 2, but 15, surfaces to be considered.

There are a number of interactions to be included in such a calculation. These are the variation of orbital energies and orbital mixings with geometry, electron-electron repulsions giving rise to multiplet structure, spin-orbit coupling, and ligand-ligand interactions. A basis set of two-hole (d^8) functions in a strong tetrahedral field limit was chosen. These functions are denoted $|(e^n t_2^{2-n})\Gamma S\Gamma' M_{\Gamma'}\rangle$, where n = 0-2 is the number of e holes, $(2 - n)$ the number of t_2 holes, Γ the irreducible representation in T_d for the electronic state, S the spin quantum number, Γ' the representation for the spin-orbit level, and $M_{\Gamma'}$ the real component of Γ'. Matrix elements of the electron-electron repulsion and spin-orbit interactions have been tabulated by Griffith[26] in terms of the familiar parameters B, C, and $\zeta(nd)$. The ligand-ligand interactions are initially omitted, so that the results correspond to a total d-electron energy vs. geometry.

There have been many crystal-field or ligand-field calculations published[27-40] for d^2 and d^8 ions in complexes of various geometries. The reviews of Sacconi[34] and Ferguson[35] describe the earlier of these in detail. The emphasis has been on octahedral, tetrahedral, square-planar, and trigonal bipyramidal geometries; there does not appear to have been a study before ours exploring thoroughly the two-dimensional space defined by θ and Φ in Table I.

As an approximate guide to the variation of orbital energies with geometry, we carried out point-charge crystal-field calculations. We present and discuss these one-electron results

Table III. Symmetry Correlations for Complexes with Two Symmetric Bidentate Ligands

T_d (ref)[a]	D_{2d}	D_2	D_{2h}
A. No Spin-Orbit Coupling			
Bending (Twisting) E(ϵ) Mode of T_d or B_1 of D_{2d}			
$^3T_1$	^3E	$^3B_2 + {}^3B_3$	$^3B_{2g} + {}^3B_{3g}$
	$^3A_2$	$^3B_1$	$^3B_{1g}$
$^1A_1$	$^1A_1$	^1A	^1A_g
B. With Spin-Orbit Coupling			
Bending (Twisting) E(ϵ) Mode of T_d or B_1 of D_{2d}			
$^3T_1$ ($J = 2$) T_2	$B_2 + E$	$B_1 + B_2 + B_3$	$B_{1g} + B_{2g} + B_{3g}$
E	$A_1 + B_1$	2A	$2A_g$
($J = 1$) T_1	$A_2 + E$	$B_1 + B_2 + B_3$	$B_{1g} + B_{2g} + B_{3g}$
($J = 0$) A_1	A_1	A	A_g
$^1A_1$	A_1	A	A_g

[a] For reference only.

Table IV. Symmetry Correlations for Complexes with One Symmetric Bidentate Ligand and Two Unidentate Ligands

T_d(ref)[a]	D_{2d}(ref)[a]	C_{2v}[b]	C_2	C_{2v}[c]	D_{4h}(ref)[a]
A. No Spin-Orbit Coupling, Twisting Mode about z					
$^3T_1$	^3E	$^3B_1$	^3B	$^3B_1$	$^3A_{2g}$
		$^3B_2$	^3B	$^3B_2$	^3E_g
	$^3A_2$	$^3A_2$	^3A	$^3A_2$	
$^1A_1$	$^1A_1$	$^1A_1$	^1A	$^1A_1$	$^1A_{1g}$
B. With Spin-Orbit Coupling, Twisting Mode about z					
$^3T_1$ T_2	$B_2 + E$	$A_1 + B_1 + B_2$	$A + 2B$	$A_1 + B_1 + B_2$	$B_{2g} + E_g$
E	$A_1 + B_1$	$A_1 + A_2$	2A	$A_1 + A_2$	$A_{1g} + B_{1g}$
T_1	$A_2 + E$	$A_2 + B_1 + B_2$	$A + 2B$	$A_2 + B_1 + B_2$	$A_{2g} + E_g$
A_1	A_1	A_1	A	A_1	A_{1g}
$^1A_1$ A_1	A_1	A_1	A	A_1	A_{1g}

[a] For reference only. [b] Nonplanar C_{2v} structure. [c] Planar C_{2v} structure.

before presenting the two-hole multiplet results. This model has several features which make it more appealing than more sophisticated and flexible molecular orbital models, namely, that the coefficients in the expansion of the electrostatic potential in terms of spherical harmonics are determined simply from the assumed molecular structure, and that the remaining parameters $\langle r^2\rangle$ and $\langle r^4\rangle$, which are expectation values of powers of the electron distance over an *nd* radial wave function, needed for calculating energy splittings of d orbitals may be chosen empirically to yield a good fit to observed spectra. It has, however, been noted[41] that parameters thus chosen are far from values calculated from ab initio atomic wave functions. Nevertheless, the transferability of empirical parameters maintains the usefulness of the model.

Our chosen parameters are $\langle r^2\rangle = 3a_0^2$ and $\langle r^4\rangle = 50a_0^4$, where a_0 is the Bohr radius; these are close to the values of 3.0 and 55.6, respectively, obtained by Day[41] in a fit to the spectra of Cu(II) bromides. A metal-ligand distance of $3.5a_0$, a ligand charge of -1 (units of e), and a spin-orbit parameter $\zeta(nd)$ ranging from 0 to 23 kcal/mol (1 eV) complete the list. A FORTRAN computer program was written to set up and diagonalize the matrix of crystal-field interactions and spin-orbit coupling for arbitrary molecular geometry of a ML_4 complex. The crystal-field matrix elements are generated by the method outlined by Griffith.[26] Figure 4 displays (left panel) the results with $\zeta(nd) = 0$ as a function of the compression angle θ on the range $\theta = \pi/4$ to $\pi/2$ with $\Phi = \pi/4$; the symmetry is in general D_{2d}, but is T_d for $\theta = \cos^{-1}(3^{-1/2})$, denoted by the dashed vertical line, and D_{4h} for $\theta = \pi/2$. Griffith's orbital notation[26] $\theta = 3z^2 - r^2$, $\epsilon = x^2 - y^2$, $\xi = yz$, $\eta =$

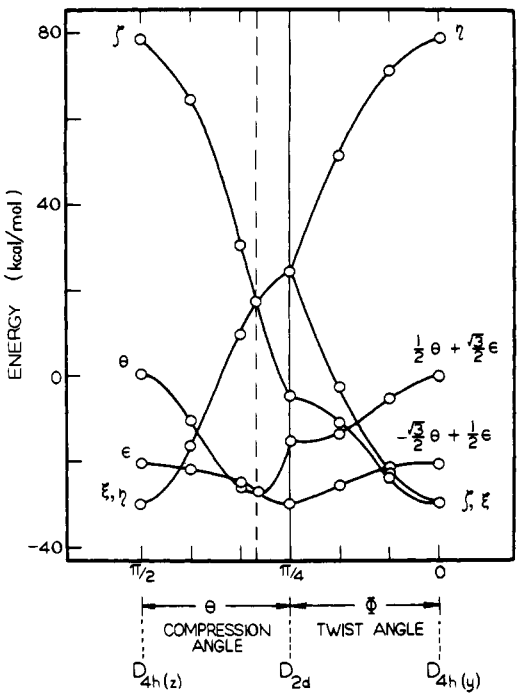

Figure 4. Crystal-field energy in kcal/mol vs. compression angle θ (left half) and vs. twist angle Φ (right half) for one-electron levels of D_2 complex. Levels are labeled by Griffith's notation.[26]

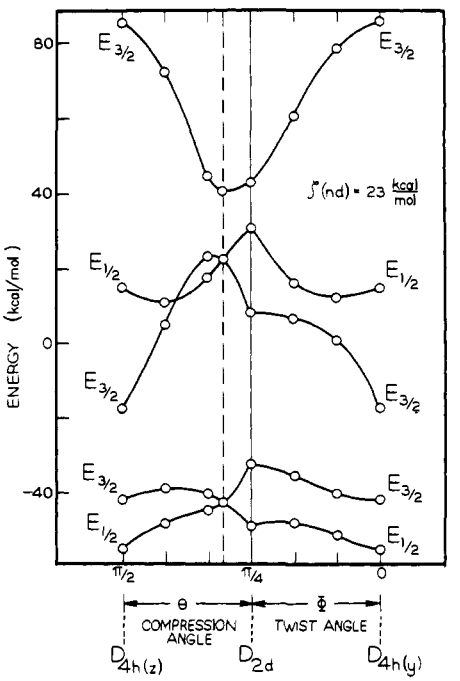

Figure 5. Crystal-field energy vs. geometry for one-electron levels of D_2 complex as in Figure 4, but with spin-orbit $\zeta(nd)$ = 23 kcal/mol = 1 eV.

xz, and $\zeta = xy$ is used to label the curves. Shown in the same figure (right panel) are the results as a function of the twist angle Φ with $\theta = \pi/4$; the two panels join at $\theta = \Phi = \pi/4$, but the slopes of the curves are in general discontinuous at this point. The leftmost structure is D_{4h} with z the C_4 axis, while the rightmost structure is D_{4h} with y the C_4 axis, so that the orbital designations differ. The most interesting feature is perhaps the strong Jahn-Teller splitting of the ξ, η pair in D_{2d} symmetry as Φ changes from $\pi/4$ to 0. One component of this high-energy pair actually becomes a component of the degenerate low-energy pair in the D_{4h} limit.

Similar calculations were performed with $\zeta(nd)$ = 1.86 kcal/mol, the approximate gaseous Ni(II) value. To the scale of Figure 4 the changes were slight and consisted mostly of the first-order splitting of the t_2 level in T_d symmetry and of the e and e_g levels in D_{2d} and D_{4h} symmetries. We show instead in Figure 5 results obtained using a much larger $\zeta(nd)$ value of 23 kcal/mol = 1 eV, a reasonable upper limit to the spin-orbit parameter for a Pt(II) complex. The arrangement by structures is the same as in Figure 4. The $j = 3/2$ level of a free ion spans irreducible representations $G_{3/2}$ in T_d, $E_{1/2} + E_{3/2}$ in D_{2d}, $E_{1/2g} + E_{3/2g}$ in D_{4h}, and $2E_{1/2}$ in D_2, while the $j = 5/2$ level spans $E_{5/2} + G_{3/2}$ in T_d, $E_{1/2} + 2E_{3/2}$ in D_{2d}, $E_{1/2g} + 2E_{3/2g}$ in D_{4h}, and $3E_{1/2}$ in D_2. Thus the crystal-field components of these levels are noncrossing in D_2, but the $E_{1/2}$ and $E_{3/2}$ components in D_{2d} may cross. We also note that the gap between the highest occupied orbital and the lowest unoccupied orbital of a d^8 complex changes from 70.9 kcal/mol for a D_{4h} complex to 12.3 kcal/mol for a D_{2d} complex (θ constant at $\pi/4$). The corresponding change with $\zeta(nd) = 0$ is from 70.6 kcal/mol to 0 (degeneracy occurring for D_{2d}). Nevertheless the 12.3 kcal/mol gap for a D_{2d} complex is sufficient to let us predict that a four-coordinated complex of Pt(II) should be diamagnetic *at any twist angle*, so that a susceptibility measurement becomes a poor structural tool for d^8 complexes with very large $\zeta(nd)$.

We now present the analogous two-hole multiplet results using electron-electron repulsion parameters of B = 1080 cm^{-1} = 3.1 kcal/mol and C = 4830 cm^{-1} = 13.8 kcal/mol, which are the Ni(II) free-ion values.[42] In Figure 6 we show the energies vs. twist angle Φ with θ fixed at $\pi/4$ for the 15 levels of symmetry A as in eq 6. The curves in Figure 6 were drawn through points obtained from calculations made at 12 values of Φ ranging from 0 to $\pi/4$. Since $\zeta(nd) = 0$, the actual symmetries are

$$\Gamma(D_2) = 6(^1A) + 3(^3B_1) + 3(^3B_2) + 3(^3B_3) \qquad (8)$$

The number of levels is 15 since we include in eq 8 only the $M_s = 0$ component of each spin-triplet. While no spin-singlets cross, there are several crossings of spin-triplets. As with the one-electron results in Figures 4 and 5, the metal-ligand bond length is taken to be $3.5a_0$ and the ligand charge to be −1. Note that as in the right-hand panels of Figures 4 and 5 the D_{4h} structure with $\Phi = 0$ has y, not z, as its fourfold axis. Features of interest include the *first-order* Jahn-Teller splittings of the D_{4h} ^3E_g multiplets, the low energy of the D_{4h} $^3B_{2g}$ multiplet (7.8 kcal/mol above $^1A_{1g}$ in this parametrization), and the symmetry of the lowest spin-singlet in D_{2d} symmetry ($^1B_1$, not $^1A_1$, although it correlates to $^1A_{1g}$ in D_{4h} via the Φ twist). The inclusion of ligand-ligand repulsions would raise the D_{4h} side relative to the D_{2d} side of the diagram; point-charge repulsions of unit ligand charges lead to an 18.8 kcal/mol destabilization of D_{4h} relative to D_{2d} with a bond length of $3.5a_0$ (1.85 Å). Thus the horizontal curve connecting the lowest ^3E_g of D_{4h} to $^3A_2$ of D_{2d} would become approximately cosine in form, with a minimum at the D_{2d} symmetry. This destabilization scales simply as the reciprocal of the bond length. Of direct interest to the spin equilibration kinetics discussed in detail in the second article[13] are a number of singlet-triplet crossings at the bottom of the diagram around $\Phi = \pi/6$ (30°), corresponding to a dihedral angle of $\pi/3$ (60°). These crossings occur at an energy of approximately 45 kcal/mol (neglecting ligand-ligand repulsions) above the D_{4h} minimum. It should be noted that spin-orbit coupling in D_{4h} symmetry mixes $^1A_{1g}$ with ^3E_g and $^3A_{2g}$, but not with $^3B_{2g}$.

Three additional series of calculations were made again with Φ as the variable, but with R = 3.0, 4.0, and $4.5a_0$, respectively. The $^1A_{1g}$ state was found to be 67.2 kcal/mol *below* $^3B_{2g}$ for the D_{4h} structure with $R = 3.0a_0$, but to be 19.2 and 32.4

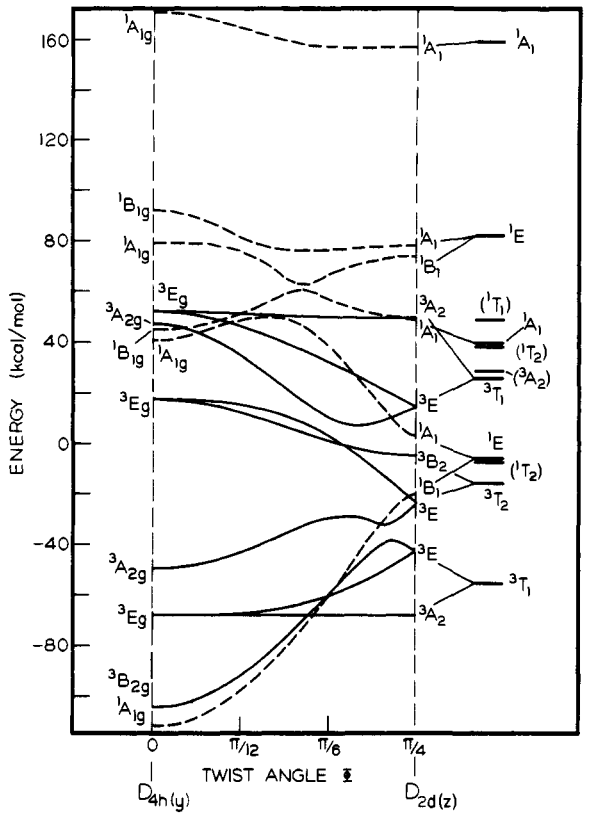

Figure 6. Energy in kcal/mol vs. twist angle Φ with θ fixed at $\pi/4$ for two-hole multiplets. Dashed curves denote spin-singlets, while solid curves denote spin-triplets. Shown only are the 15 multiplets which contain levels transforming as symmetry A in the group D_2 when spin-orbit coupling is introduced [$\zeta(nd) = 0$ here]. Not shown are the additional multiplets transforming in the group D_{4h} as $^1A_{2g}$, $^1B_{2g}(2)$, $^1E_g(3)$, and $^3B_{1g}$, as these do not contain spin-orbit levels of symmetry A in the group D_2. For reference purposes *all* multiplets for a T_d species are shown to the right of the figure, with tie lines drawn to the D_{2d} energies for those levels considered in the low symmetry. The electron-electron repulsion parameters are $B = 3.1$ and $C = 13.8$ kcal/mol, respectively.

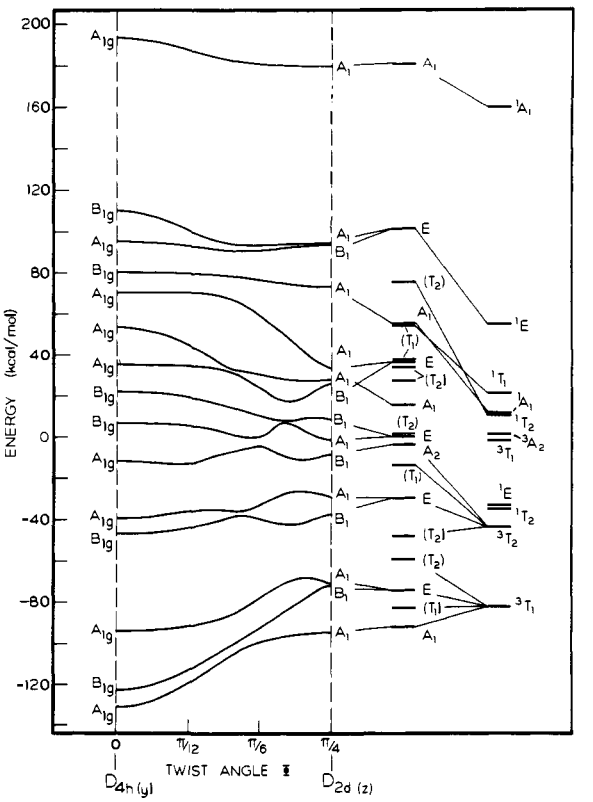

Figure 7. Two-hole multiplet energies as in Figure 6, but with $\zeta(nd) = 23$ kcal/mol = 1 eV. The 15 curves represent the 15 levels of symmetry A in the group D_2.

kcal/mol *above* with $R = 4.0$ and $4.5a_0$, respectively. Thus this energy difference is a sensitive function of the bond length, with the crossover occurring for $R = 3.6a_0$. In the limit $R \rightarrow \infty$, the $^1A_{1g}$ and $^3B_{2g}$ terms correlate to ^1D and ^3F, respectively, separated by $5B + 2C = 43.1$ kcal/mol. For the D_{2d} structures ($\theta = \pi/4$) the $^3A_2$ term arising from ^3F lies below the lowest spin singlet, namely, $^1B_1$ from ^1D, over the entire range of R from $3.0a_0$ to infinity. An additional series of calculations was made for the D_{4h} structure only with R fixed at $2.83a_0$ (1.50 Å) and with the point charges replaced by point *dipoles* ranging in strength from 0 to 5 au. The results as expected essentially matched those reported by Maki,[27] although we used a slightly different electron repulsion parametrization. It should be noted that variation of charge or dipole strength at fixed R is not the same as the variation of R at fixed charge or dipole strength, as the latter variation is accompanied by a changing balance between the $L = 2$ and $L = 4$ terms in the crystal-field expansion.

Figure 7 presents results similar to those in Figure 6, but with $\zeta(nd) = 23$ kcal/mol = 1 eV. As in Figure 5, the very large $\zeta(nd)$ value was chosen so as to magnify the effects of spin-orbit coupling. We now note the numerous avoided crossings, and the smooth correlation of the ground levels of D_{4h} and D_{2d} symmetries. The results shown in Figure 8 are like those in Figure 6, with $\zeta(nd) = 0$, but are a function of the compression angle θ at a fixed value of $\Phi = \pi/4$. The curves were drawn through points obtained from calculations made at nine values of θ. This last diagram is the one most nearly like the qualitative correlation diagram given by Whitesides,[17] but it is not the one appropriate to the twisting motion presumably responsible for the isomerization in complexes of the Ni(L-L)X_2 and Ni(L-L)$_2$ types. In Figure 8 we note the crossings near $\theta = 0.39\pi$ (70°) and the expected extra degeneracies at $\theta = \theta_0$, corresponding to T_d symmetry. Were the remaining 30 levels to be included in Figures 6-8, there would be quite a thicket of curves!

IV. Summary

A series of theoretical studies of the kinetics of the equilibration of planar spin-singlet and tetrahedral spin-triplet complexes of Ni(II) is begun by the introduction of global bending coordinates for four-coordinate species. These coordinates (Table I and Figures 1-3) provide an attractive framework within which to visualize the structural interconversions. In particular they clearly show the multiplicity of possible paths connecting planar and tetrahedral structures for complexes with four unidentate ligands. Potential energy surfaces for singlet and triplet levels are calculated both with and without spin-orbit coupling as a function of these coordinates using a crystal-field model. The results are used to illustrate the types of features that would occur in MX_4, M(L-L)X_2, and M(L-L)$_2$ complexes of d^8 ions, and are not meant to represent quantitatively the energy levels in a given complex. Indeed the parametrization (bond length, ligand charge, and $\langle r^n \rangle$ values) used obtaining the results shown in Figures 4-8 corresponds to a very strong metal-ligand interaction. This is seen most clearly in Figure 4, where the orbital splitting for the T_d structure corresponds to 10 Dq (or Δ) equal to $-15\,480$ cm^{-1}. A calculation with the same parameters for an octahedral ML_6 complex thus yields a 10 Dq value of $-\frac{9}{4}$ times the above, or 34 830 cm^{-1}, which is excessive for Ni(II) although possibly not for Pt(II). Thus it is not surprising that Figures 6 and 8 show excessively large "activation energies"

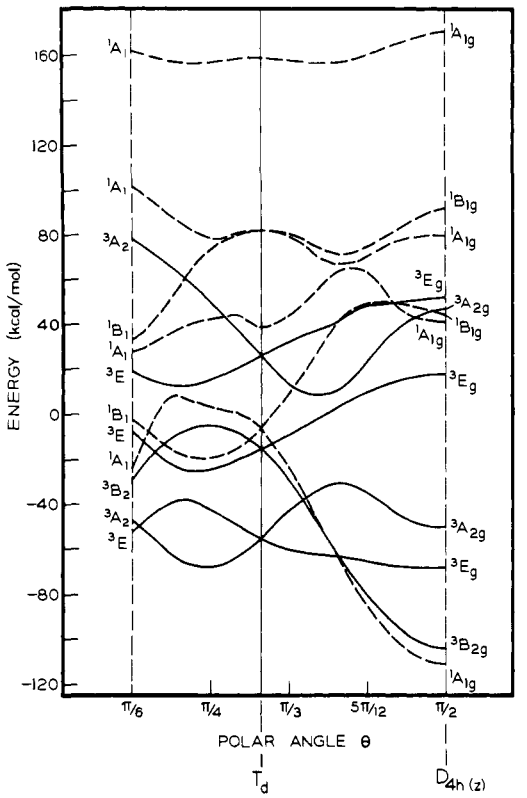

Figure 8. Two-hole multiplet energies as in Figure 6 with $\zeta(nd) = 0$, but vs. the compression angle θ with Φ at $\pi/4$. As in Figure 6 the dashed curves denote spin-singlets and solid curves denote spin-triplets. Again shown only are the 15 multiplets which contain levels transforming as symmetry A in the group D_2 when spin-orbit coupling is introduced.

of approximately 45 kcal/mol for the crossing of singlet and triplet curves. However, these energies would be reduced both by the inclusion of suitable ligand-ligand interactions favoring a tetrahedral structure and by adjustment of the crystal-field parameters to reflect more accurately the metal-ligand interactions to be expected in complexes of interest. Such crossings, which become anticrossings when spin-orbit coupling is introduced, provide the basis for the spin-change "hoppings" treated in detail in the second article[13] of this series.

It is appropriate to comment further on the nature of the potential energy surface intersections. States of the same spin and spatial symmetry may have the same energy at *points* in θ, Φ space or over an s-2 dimensional domain in the space of all s internal coordinates, while states of different spin or orbital symmetry may have the same energy along a *line* in θ, Φ space, or in general over an s-1 dimensional domain.[43,44] If spin-orbit coupling is considered, the dimensionality of the intersection subspaces is in general reduced by one for states of the same combined spin and orbital symmetry, but remains s-1 for states of different combined symmetry. However, conical intersections of the surfaces in θ, Φ space for any two of the 15 states of combined symmetry A in the point group D_2 cannot be excluded, since in this case the imaginary parts of the off-diagonal spin-orbit matrix elements are zero for all θ and Φ.

Acknowledgments. The author wishes to thank The University of Michigan Computing Center for use of the Amdahl 470V/6 computer and Mr. Peter G. Sherman for writing the one-electron part of the crystal-field program.

References and Notes

(1) R. H. Holm and M. J. O'Connor, *Prog. Inorg. Chem.*, **14**, 241-401 (1971).
(2) R. H. Holm and C. J. Hawkins, "NMR of Paramagnetic Molecules: Principles and Applications", G. N. LaMar, W. DeW. Horrocks, Jr., and R. H. Holm, Ed., Academic Press, New York, N.Y., 1973, pp 243-332.
(3) L. H. Pignolet and G. N. LaMar in ref 2, pp 333-369.
(4) L. H. Pignolet, *Top. Curr. Chem.*, **56**, 91 (1975).
(5) R. H. Holm, "Dynamic Nuclear Magnetic Resonance Spectroscopy", L. M. Jackman and F. A. Cotton, Ed., Academic Press, New York, N.Y., 1975, pp 317-376.
(6) G. R. Van Hecke and W. D. Horrocks, Jr., *Inorg. Chem.*, **5**, 1968 (1966).
(7) L. H. Pignolet and W. D. Horrocks, Jr., *J. Am. Chem. Soc.*, **91**, 3976 (1969).
(8) G. N. Lamar and E. O. Sherman, *Chem. Commun.*, 809 (1969).
(9) G. N. Lamar and E. O. Sherman, *J. Am. Chem. Soc.*, **92**, 2691 (1970).
(10) L. H. Pignolet, W. D. Horrocks, Jr., and R. H. Holm, *J. Am. Chem. Soc.*, **92**, 1855 (1970).
(11) L. Que and L. H. Pignolet, *Inorg. Chem.*, **12**, 156 (1973).
(12) J. J. McGarvey and J. Wilson, *J. Am. Chem. Soc.*, **97**, 2531 (1975). The ligand abbreviated "dpp" is 1,3-bis(diphenylphosphino)propane.
(13) L. L. Lohr, Jr., and E. K. Grimmelmann, *J. Am. Chem. Soc.*, following paper in this issue.
(14) B. R. McGarvey, *J. Am. Chem. Soc.*, **94**, 1103 (1972); also see R. J. Kurland and B. R. McGarvey, *J. Magn. Reson.*, **2**, 286 (1970).
(15) R. B. Woodward and R. Hoffmann, "The Conservation of Orbital Symmetry", Academic Press, New York, N.Y., 1970, and references cited therein.
(16) D. R. Eaton, *J. Am. Chem. Soc.*, **90**, 4272 (1968).
(17) T. H. Whitesides, *J. Am. Chem. Soc.*, **91**, 2395 (1969).
(18) For example see M. A. Hoselton, R. S. Drago, L. J. Wilson, and N. Sutin, *J. Am. Chem. Soc.*, **98**, 6967 (1976), and references cited therein.
(19) M. Born and J. R. Oppenheimer, *Ann. Phys. (Leipzig)*, **84**, 457 (1927).
(20) S. Y. Wang and L. L. Lohr, Jr., *J. Chem. Phys.*, **60**, 3901, 3916 (1974); **61**, 4110 (1974); **62**, 2013 (1975).
(21) L. S. Bartell and R. M. Gavin, Jr., *J. Chem. Phys.*, **48**, 2466 (1968).
(22) For example, see J. S. Koehler and D. M. Dennison, *Phys. Rev.*, **57**, 1006 (1940).
(23) K. S. Pitzer and L. S. Bernstein, *J. Chem. Phys.*, **63**, 3849 (1975).
(24) E. B. Wilson, Jr., J. C. Decius, and P. C. Cross, "Molecular Vibrations", McGraw-Hill, New York, N.Y., 1955, pp 312-340.
(25) G. Herzberg, "Molecular Spectra and Molecular Structure. III. Electronic Spectra and Electronic Structure of Polyatomic Molecules", Van Nostrand, Princeton, N.J., 1966, pp 563-579.
(26) J. S. Griffith, "The Theory of Transition Metal Ions", Cambridge University Press, New York, N.Y., 1961.
(27) G. Maki, *J. Chem. Phys.*, **28**, 651 (1958); **29**, 162, 1129 (1958).
(28) A. D. Liehr and C. J. Ballhausen, *Ann. Phys. (N.Y.)*, **6**, 134 (1959).
(29) C. J. Ballhausen and A. D. Liehr, *Mol. Phys.*, **2**, 123 (1959).
(30) R. F. Fenske, D. S. Martin, Jr., and K. Ruedenberg, *Inorg. Chem.*, **1**, 441 (1962).
(31) D. S. Martin, Jr., M. A. Tucker, and A. J. Kassman, *Inorg. Chem.*, **5**, 1298 (1966).
(32) M. Ciampolini, *Inorg. Chem.*, **5**, 41 (1966).
(33) M. J. Norgett, J. H. M. Thornley, and L. M. Venanzi, *J. Chem. Soc.*, 540 (1967).
(34) L. Sacconi, "Transition Metal Chemistry", Vol. 4, R. L. Carlin, Ed., Marcel Dekker, New York, N.Y., 1968, pp 113-198.
(35) J. Ferguson, *Prog. Inorg. Chem.*, **12**, 159 (1970).
(36) J. C. Hempel, J. C. Donini, B. R. Hollebone, and A. B. P. Lever, *J. Am. Chem. Soc.*, **96**, 1693 (1974).
(37) J. C. Donini, B. R. Hollebone, G. London, A. B. P. Lever, and J. C. Hempel, *Inorg. Chem.*, **14**, 455 (1975).
(38) H. Isci and W. R. Mason, *Inorg. Chem.*, **14**, 905 (1975).
(39) I. Bertini, D. Gatteschi, and A. Scozzafava, *Inorg. Chem.*, **15**, 203 (1976).
(40) T. G. Harrison, H. H. Patterson, and M. T. Hsu, *Inorg. Chem.*, **15**, 3018 (1976).
(41) P. Day, *Proc. Chem. Soc., London*, 18 (1964).
(42) Reference 26, p 437.
(43) E. Teller, *J. Phys. Chem.*, **41**, 109 (1937).
(44) A. J. Stone, *Proc. R. Soc. London, Ser. A*, **351**, 141 (1976).